

# A Realistic Particle Physics Dark Energy Model

A. de la Macorra

*Instituto de Física, UNAM, Apdo. Postal 20-364, 01000 México D.F., México*

We present a realistic dark energy model derived from particle physics. Our model has essentially no free parameters and has an equivalent fit to the observational data (CMB, SN1a and LSS) as LCDM and a better fit than the best effective  $w(z)$  model. With the lack of a clear determination of the cosmological parameters theoretical considerations should be taken seriously to distinguish between dark energy models.

Recent cosmological observations [1]-[3] imply the universe is dominated by a dark energy fluid. However, there is no theoretical understanding what this dark energy is. The simplest and most common assumption is a cosmological constant model. Comparing LCDM to wmap, SN1a and LSS data one finds a large degeneracy among the cosmological parameters  $P_6 = (H_o, \Omega_{DE}, \Omega_b h^2, \tau, n_s, A_s)$  [4]-[6]. Several attempts have been made to infer from the data the best dark energy model by parameterizing the equation of state parameter  $w(z)$  as a function of redshift  $z$  [5]. The analysis shows that the degeneracy of the cosmological parameters  $P_6$  remains but the central values varies. The best fit model for a dynamical  $w(z)$  and LCDM have an equivalent  $\chi^2/dof = 1.08$  value [4],[5] but LCDM has a better Akaike or Bayesian information criteria [5]. With the lack of a clear determination of  $P_6$  theoretical considerations should be taken seriously to distinguish between dark energy models.

Even though the LCDM model has a good fit to the cosmological data it is hard to accept it from a theoretical point of view. It does not answer some fundamental questions as where it comes from and why does it have at present time an energy of the same order of magnitude as dark matter, i.e. the coincidence problem. From a theoretical point of view we would like to have a dark energy model which is well motivated from particle physics, answers the fundamental question which a LCDM does not and has at least an equivalent fit to the data. The best theoretical model should have the least number of free parameters and should give reasonable explanations and values for them.

In this work we will present a realistic dark energy model derived from particle physics. We will show that this model has, indeed, an equivalent fit to the observational data as LCDM. It has essentially no free parameters so the cosmological  $P_6$  quantities are the only free parameters. For most of the cosmological time the energy density is proportional to radiation since the particles are massless. It is the dynamics of the model that give rise to a late time phase transition at a scale  $\Lambda_c = O(10-100eV)$  and an effective scalar field appears which gives the dark energy today. For energies larger than  $\Lambda_c$  the particles are massless and redshift as radiation and below  $\Lambda_c$  the particles acquire a non-perturbative mass. The model is based on gauge theory and has an equivalent structure as the well established standard model of particle physics.

The dark energy gauge group gives an effective potential of the form  $V \propto \phi^{-n}$ , where  $\phi$  is the dark energy (quintessence field) and the power  $n$  is fixed by the number of fields. Inverse power law potentials "IPL" were first introduced by [7] and [8] to use ADS superpotentials [9] to get an effective IPL potential. However, the models of [7] had no particle physics interpretation and the models of [8] had  $n > 2$  and are phenomenological not viable. We were the first ones to study phenomenological acceptable ADS superpotentials giving an IPL with  $n < 2$  and our model has  $n = 2/3$  [10]. We would like to emphasize the following theoretical points of our model:

- The potential is calculated from our best theoretical theories, i.e. gauge theories
- The superpotential is exact and the potential is stable against quantum corrections
- The appearance of quintessence field is due to a late time phase transition given by  $\Lambda_c$
- The condensation scale  $\Lambda_c$  is determined by first principles (it is given in terms of the number of fields)
- The initial energy is given also only by the number of fields
- The number of fields is determined by imposing gauge coupling unification
- The solution is an attractor even though the quintessence field has not reached it yet
- Our dark energy model has no free parameters
- It has an equivalent fit to the observational data (CMB and SN1a) as the best fit model
- It "solves" the coincidences problem

This last point is due to a late time phase transition. The onset of the quintessence field is at about matter-radiation equality since the scale factor  $a_c$  (i.e. at  $\Lambda_c$ ) is in cosmological times very close to matter-radiation equality  $a_{eq}$  ( $a_c/a_{eq} \simeq 10^{-2}$ ). This means that  $\rho_{DG}/\rho_r$  is constant from the end of inflation  $a_{inf} \simeq 10^{-30}$  until  $a_c \simeq 10^{-6}$  which accounts for most of the time.

The dark energy model is simply a  $SU(N_c = 3)$  gauge group with  $N_f = 6$  elementary particles in the fundamental representation and with only gravitational interaction with the standard model of particle physics. The phase transition scale  $\Lambda_c$  is determined only by  $N_c$  and  $N_f$  and the value of the gauge coupling constant at some arbitrary energy scale. Motivated by string theory our dark energy model is constrained to be unified with the standard model gauge groups at the unification scale. For viable cosmological models gauge cou-

pling unification determines the values of  $N_c, N_f$  [10]. With this non-trivial constrained the evolution of the gauge coupling constant and  $\Lambda_c$  are completely fixed. At high energies the dark elementary fields are massless and  $\rho_{DG} \propto a^{-4}$ ,  $\rho_{DG}/\rho_r$  is constant and the ratio is given only in terms of the number of particles (c.f. eq.(2)). At lower energies a phase transition takes place due to a strong gauge coupling constant. At this scale the dark elementary fields are bind together producing gauge invariant states. The relevant scale for this process is the condensation scale  $\Lambda_c$  and for a gauge group  $SU(N_c)$  with  $N_f$  matter fields in susy is given by the one-loop renormalization group equation  $\Lambda_c = \Lambda_{gut} e^{-8\pi^2/b_o g_{gut}^2}$  where  $b_o = 3N_c - N_f$  is the one-loop beta function and  $\Lambda_{gut} \simeq 10^{16} \text{GeV}$ ,  $g_{gut} \simeq \sqrt{4\pi/25.7}$  are the unification energy scale and coupling constant, respectively. In our dark energy model we have  $N_c = 3, N_f = 6$  giving  $b_o = 3$  and  $\Lambda_c = 42 \text{eV}$ . Strong gauge interactions produce a non-perturbative potential  $V$ . This potential can be calculated using ADS potential [9]. The superpotential for a non-abelian  $SU(N_c)$  gauge group with  $N_f$  massless fields is  $W = (N_c - N_f)(\Lambda_c^{b_o}/\det(Q\tilde{Q}))^{1/(N_c-N_f)}$ . The scalar potential in susy for one dynamical meson field  $\phi$ , the pseudo-Goldstone boson, is  $V = e^{\phi^2/2}|W_\phi|^2$  with  $W_\phi = \partial W/\partial\phi$ , giving [8],[10]

$$V = c^2 \Lambda_c^{4+2/3} e^{\phi^2/2} \phi^{-2/3} \quad (1)$$

with  $c = 2N_f = 12$ . We have included the exponential factor in eq.(1) because once gravity is taken into account it gives the correct normalization in the Einstein frame. For values of the field much smaller than the Planck mass  $m_p = 2.4 \cdot 10^{18} \text{GeV} \equiv 1$  the exponent term is irrelevant but for  $\phi \simeq 1$  it gives a (small) correction. The evolution is basically determined by the inverse power law exponent  $\phi^{-2/3}$ . In order to study the evolution of eq.(1) the initial condition on  $\phi$  must be set and the only natural initial value is  $\phi_i = \Lambda_c$  since it is precisely  $\Lambda_c$  the relevant scale of the physical binding process. The potential in eq.(1) has a minimum at  $\phi = \sqrt{n} = \sqrt{2/3}$  and the value of the potential is  $V|_{min} = c^2 \Lambda_c^{4+2/3} e^{1/3} (3/2)^{1/3}$ . The evolution of  $\phi$  with different initial conditions is shown in fig.2. Even though the evolution of  $\phi$  depends on  $\Omega_{\phi i}$  its value at present time  $a_o = 1$  is (almost) independent of the initial conditions. Global symmetries and susy protect the mass of the quintessence field  $\phi$ . In fact the ADS superpotential is exact and receives no corrections [9]. The only radiative corrections arise due to the Kahler potential. However, our model is stable against radiative corrections [11], the shape of the potential remains the same and the v.e.v. of  $\phi$  suffers a small shift but this does not affect the cosmological predictions since the solution is an attractor. The complete evolution of the dark energy group can be seen in fig.1. Notice that  $\rho_{DG}$  tracks radiation for a long period of time, including nucleosynthesis "NS" epoch, since all the particles are massless and the onset of the quintessence field is at a very late time ( $a_c \simeq 10^{-6}$ ) and close to matter-radiation equality

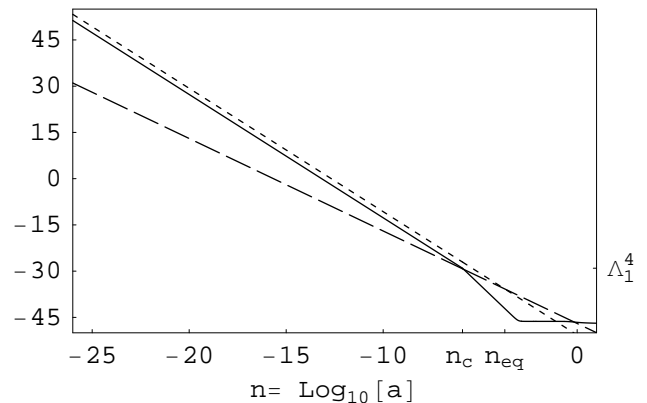


FIG. 1: We show the evolution of  $\rho_r, \rho_m$  and  $\rho_{DG}$  (dotted, dashed and solid lines, respectively) as a function of  $\text{Log}_{10}(a)$  with  $a_o = 1$  with no extra degrees of freedom, i.e.  $g_h = 0$ . The value of equivalence is  $n_{eq} = -3.6$  while the phase transition takes place at  $n_c = -5.9$ .

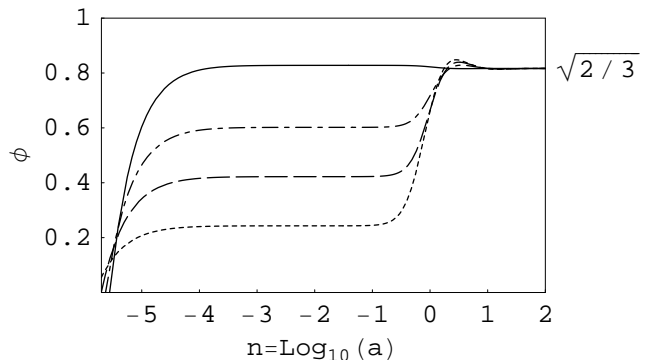


FIG. 2: We show the evolution of  $\phi$  for different initial conditions  $\Omega_{DGi} = 0.01, 0.03, 0.06, 0.11$  (dotted, dashed, dot-dashed and solid lines, respectively).

( $a_{eq} \simeq 10^{-4}$ ). The fact that  $\Lambda_c$  is so small and the appearance of the quintessence field is at such a late time "solves" the coincidence problem since it implies that an accelerating universe will necessarily be at a scale factor larger than  $a_c$  and  $a_{eq}$ , close to present time. In our case the scalar field is present only at  $a \geq a_c$  and it does not track the background at all, as can be seen from figs.1,3 and 4.

The total energy density of the universe is given  $\rho_T = \rho_{sm} + \rho_{DG} + \rho_h$ , where  $\rho_{sm}$  is the energy density of the standard model (we will take it as the minimal supersymmetric standard model) and we have allowed for  $\rho_h$  hidden particles which could be present at earlier times. Examples of these particles are the ones requires to break susy in the standard model and are widely predicted by string theory. The only constrained we imposed to  $\rho_h$  is that they do not contribute to the present day energy density nor at NS. One important constrained on the energy density at earlier times is given at NS. The extra amount of relativistic energy density at NS is usually pa-

parameterized by an effective neutrino  $\Delta N_\nu \leq 0.2 - 0.3$  which implies an upper bound  $\Omega_{ex}(NS) \leq 0.045$  in the most stringent case and  $\Omega_{ex}(NS) \leq 0.09$  at two  $\sigma$  [12]. However, NS is still fine with  $\Delta N_\nu \leq 4.1$  which implies a bound  $\Omega_{ex}(NS) \leq 0.4$  if new physics is involved at that time (as neutrino asymmetry) [13].

Our dark energy model has no free parameter, however, the total energy density could in principle contained more particles than the standard model and our dark group, i.e.  $g_h \neq 0$ . In fact extra particles would be needed to break susy in the visible sector. To simplify the discussion we will assume that these particles, if present, acquire a large mass (larger than  $TeV$ ) so that they do not affect NS and that they are coupled to the standard model at high energies. Examples of this are the gauge mediated susy breaking models, extensively studied in particle physics context, which require an energy scale  $\Lambda_h = O(10^{7-8})GeV$  in order to give masses of the order of  $TeV$  to the standard model particles [14]. Since the hidden sector is only coupled to our dark model via gravity, it will induce a susy breaking to the dark group of the order  $m_s = \Lambda_h^3/m_p^2$  which is smaller than  $\Lambda_c$  and does, therefore, not affect the running of the gauge coupling and the onset of our potential given in eq.(1). These extra particles will not contribute to the energy density at NS nor at present time but they are important for determining the ratio of temperature between the standard model and our dark group. The effect of these extra particles is to decrease the ratio of the temperature and  $\Omega_{DG}$ . From entropy conservations one can determine  $\Omega_{DG}$  giving [11]

$$\Omega_{DG} = \frac{g_Q(T_D/T)^4}{g_{sm} + g_Q(T_D/T)^4}, \quad \left(\frac{T_D}{T}\right) = \left(\frac{q}{g_{dec}}\right)^{1/3} \quad (2)$$

with  $q = 10.75$ ,  $g_{sm} = 10.75$  at NS and  $q = 2 \times 10.75 \times 4/11$ ,  $g_{sm} = 3.36$  at  $\Lambda_c$  and  $g_{dec} = g_{MSSM} + g_h$ , with  $g_{MSSM} = 228.75$  and  $g_h$  the degrees of freedom of the MSSM and the hidden sector, respectively. The term  $4/11$  in  $q$  at  $\Lambda_c$  takes into account for neutrino decoupling and  $10.75, 3.36$  are the relativistic degrees of freedom of the standard model at NS and at present time while  $g_Q = 97.5$  are the degrees of freedom of our model [11]. An upper bound on  $\Omega_{DG}, T_D$  can be established if there are no hidden particles,  $g_h = 0$ , and eq.(2) gives

$$\Omega_{DG}(NS) \leq 0.13 \quad \Omega_{DG}(\Lambda_c) \leq 0.11 \quad (3)$$

where  $\Omega_{DG_i}$  stands at  $\Lambda_c$ , i.e. the onset of the quintessence field. Notice that the upper limit is still within the existing NS bounds (not the most stringent one) since  $\Delta N_\nu \leq 1$  implies  $\Omega_{ex} \leq 0.14$ . For  $g_h \neq 0$  than we get a smaller  $\Omega_{DG}(NS)$  and for  $\Omega_{DG}(NS) = 0.09, 0.045$  we require  $g_h = 90, 327$ , respectively, giving  $\Omega_{DG_i} = 0.076, 0.037$ . Typical gauge mediated susy breaking models have  $g_h = O(200)$  [14]. Clearly we have no precise knowledge of how many hidden sector particles are nor how susy is broken. Furthermore, the contribution of  $g_h$  would be the same for all dark energy models

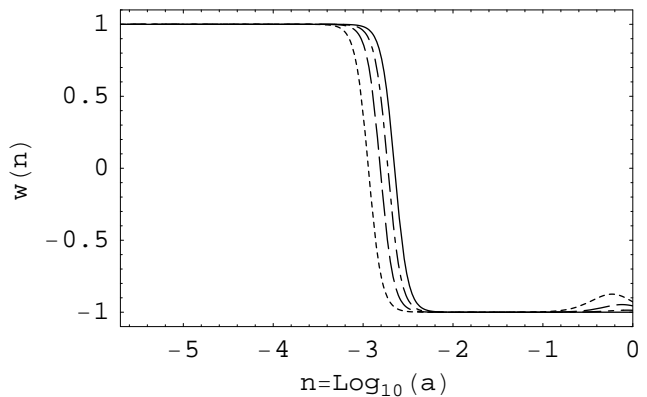


FIG. 3: We show the evolution of  $w$  as a function of  $n = \log_{10}(a)$  from  $n_c$  (i.e. at  $\Lambda_c$ ) to present day  $n_o = 0$  for different initial conditions  $\Omega_{DG_i} = 0.01, 0.03, 0.06, 0.11$  (dotted, dashed, dot-dashed and solid lines, respectively).

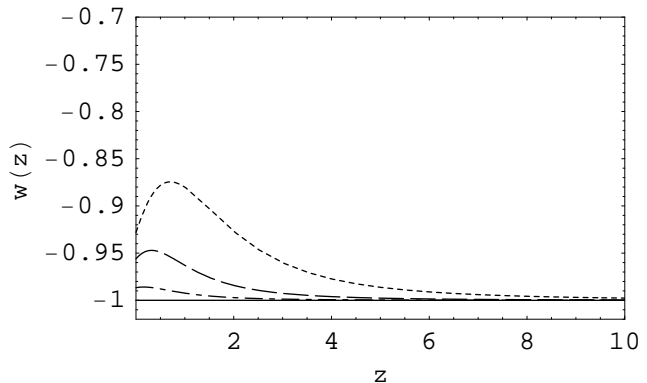


FIG. 4: We show the late time evolution of  $w$  as a function of redshift  $z$  for different initial conditions  $\Omega_{DG_i} = 0.01, 0.03, 0.06, 0.11$  (dotted, dashed, dot-dashed and solid lines, respectively).

and the uncertainty lies in the hidden sector and not on our dark group model which, as stated above, has no free parameter.

In fig.3 we show the evolution of  $w$  below  $\Lambda_c$ , i.e. for  $a > a_c$  (above  $\Lambda_c$  it is simply  $w = 1/3$ ). It has an initial kinetic period  $w = 1$  following a region with  $w = -1$ , lasting almost the same amount of e-folds as the first one, and it grows later to its present value  $w_o$ . We see that the value of  $w_o$  depends slightly on the initial conditions  $\Omega_{DG_i}$ . At equivalence  $\text{Log}_{10}[a_{eq}] \simeq -3.6$  the value of dark energy is  $\Omega_{DG} \simeq 10^{-6}$  while at last scattering ( $a \simeq 1/1090$ ) it is  $\Omega_{DG} \simeq 10^{-7}$ , quite small in both cases. In fig.4 we show how  $w$  increases as a function of redshift  $z$  for different values of  $\Omega_{DG_i}$ . In fig.5a we plot the present day values of  $w_o$  and  $w'_o \equiv \partial w / \partial z|_o$  for different initial  $\Omega_{DG_i}$  and final  $\Omega_{DG_o}$ . Notice that the variation is very small. In fact we have  $-1 < w_o < -0.92$  and  $-0.06 < w'_o < 0.19$  if  $\Omega_{DG_o}$  varies from  $0.65 \leq \Omega_{DG_o} \leq 0.75$  and  $\Omega_{DG_i} < 0.11$ . For larger  $\Omega_{DG_i} > 0.1$  we get a flat and small  $w_o$ , very close to  $-1$ , with a slightly negative  $w'_o$

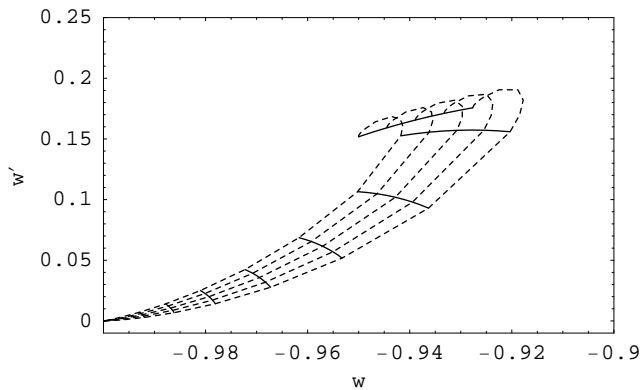


FIG. 5: We show the values of  $w$  and its derivative  $w' = \partial w / \partial z|_o$  at present time for different values of  $\Omega_{Qo}$  and  $\Omega_{DGi}$ . The dotted lines have constant  $\Omega_{Qo}$  and from bottom to top they have  $\Omega_{Qo} = 0.66, 0.68, 0.70, 0.72, 0.74$ , respectively. The solid lines have  $\Omega_{DGi}$  constant with  $\Omega_{DGi} = 0.0002, 0.01, 0.02, 0.03, 0.04, 0.05, 0.06$  from top to bottom. Notice the resulting  $w, w'$  region is very small and it has an upper limit to  $w$  and  $w'$ .

$\Omega_{DGi}$	$\Omega_{DGo}$	$\chi_{sn1a}^2$	$w_o$	$w'_o$	$z_{ac}$
0.11	0.69	177.1	-1	$-10^{-5}$	0.64
0.06	0.70	177.2	-0.99	0.01	0.67
0.03	0.71	177.4	-0.96	0.06	0.70
0.01	0.73	177.5	-0.94	0.15	0.73
LCDM	0.69	177.1	-1	0	0.65

TABLE I: We show the best fit model compared to the Golden SN1a set for different values of  $\Omega_{DGi}$  and LCDM.

while for values  $\Omega_{DGi} < 0.1$  we have a small positive  $w'_o$  and a larger  $w_o$ . As seen from fig.5a the variation is more sensitive with respect to  $\Omega_{DGi}$  than to  $\Omega_{DGo}$ . The values of  $w_o, w'_o$  are insensitive to  $H_o$ . At this point, we would like to emphasize, again, that  $\Omega_{DGi}$  is not a free parameter, we do not marginalize it, but we show the slight dependence of  $w_o, w'_o$  over it.

We now compare our model with the data. The likelihood contours for the Golden SN1a set [2] of  $\Omega_{DGi}$  vs  $\Omega_{DGo}$  are shown in fig.6. The best fit to the Golden SN1a set for different initial conditions are shown in table I. We see that for the different values of  $\Omega_{\phi i}$  we get an equivalent fit as a LCDM. The acceleration redshift (where the universe begins to accelerate) is centered around  $z_{ac} = 0.65 \pm 0.05$  with  $\chi_{sn1a}^2 < 178$ . The best fit model has a very flat  $w$  with  $-1 < w_o < -0.94$ , even though the  $\Omega_{DGi} = 0.01$  case with  $w_o = -0.94, w'_o = 0.15$  does a reasonable job.

To compare our model to the wmap data we use KINKFAST [15] (a modification of CMBFAST [16] to include a dynamical dark energy). The best fit to wmap of our dark energy model and LCDM can be seen from table II. The parameters  $n_s, \tau$  are degenerated and different values would give the same  $\chi_{tot}$  [4].

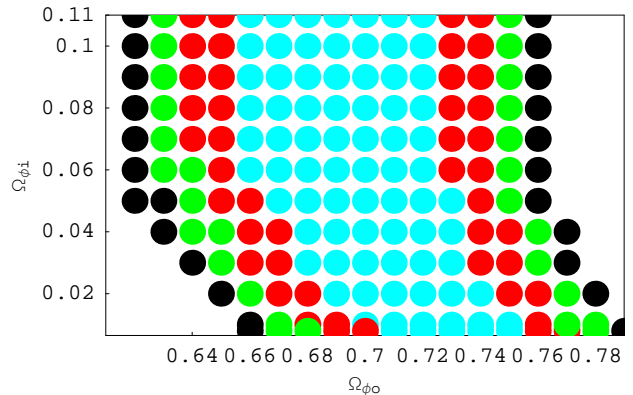


FIG. 6: We show the likelihood contours as a function of  $\Omega_{DGi}, \Omega_{Qo}$  compared to the Golden set of SN1a. We have  $\chi_{sn1a}^2 < 178, 178 < \chi_{sn1a}^2 < 179, 179 < \chi_{sn1a}^2 < 180$  and  $180 < \chi_{sn1a}^2 < 181$  (light blue, red, light green and black, respectively).

$\Omega_{DGi}$	$\Omega_{DGo}$	$\chi_{wmap}^2$	$H_o$	$w_b$	$n_s$	$\tau$	$\sigma_8$	$w_o$
0.11	0.70	1428.7	69	0.0227	0.97	0.11	0.85	-1
0.06	0.70	1428.7	69	0.0227	0.97	0.11	0.84	-0.99
0.03	0.69	1428.7	68	0.023	0.97	0.11	0.83	-0.96
0.01	0.71	1429.2	68	0.0227	0.97	0.13	0.77	-0.93
LCDM	0.70	1428.7	69	0.02327	0.97	0.11	0.84	-1

TABLE II: We show the best fit model compared to wmap data for different values of  $\Omega_{DGi}$  and LCDM.

Combining the Golden SN1a set with wmap we show in table III the best fit model for different values of  $\Omega_{DGi}$  and for the best LCDM. Notice that all four initial conditions have an equivalent fit and therefore, the data is not sensitive enough to distinguish between them. The total number of degrees of freedom is 157 for the Golden SN1a set and 1342 for the wmap data. We get for our best fit model a  $\chi_{tot}^2 = 1605.8$  with  $\chi_{tot}^2/dof = 1.08$ . The dof is the same for our dark energy model as for LCDM. It is interesting to note that after an exhaustive analysis of model independent evolution of dark energy [5] the best

$\Omega_{DGi}$	$\Omega_{DGo}$	$\chi_{wmap}^2$	$\chi_{sn1a}^2$	$\chi_{tot}^2$	$H_o$	$\tau$	$\sigma_8$	$w_o$
0.11	0.70	1428.7	177.1	1605.8	69	0.11	0.85	-1
0.06	0.70	1428.7	177.2	1605.9	69	0.11	0.84	-0.99
0.03	0.71	1428.8	177.4	1606.2	69	0.12	0.81	-0.96
0.01	0.72	1429.3	177.5	1606.8	69	0.12	0.76	-0.94
LCDM	0.70	1428.7	177.1	1605.8	69	0.11	0.84	-1

TABLE III: We show the best fit model compared to the Golden SN1a set and wmap for different values of  $\Omega_{DGi}$  and a LCDM. All models have  $n_s = 0.97, w_b = 0.0227$ . The number of degrees of freedom is the same for our dark energy model and LCDM, with a total dof  $1342+157-6= 1493$ , giving a  $\chi_{tot}^2/dof = 1.08$ .

fit model has  $\chi_{tot}^2 = 1602.9$  at the price of introducing 4 extra parameters giving the same  $\chi_{tot}^2/dof = 1.08$  but a worse Akaike or Bayesian criteria [5]. The Akaike information criteria [17] requires the smallest  $AIC = \chi_{tot}^2 + 2k$  while the Bayesian [18] has  $BIC = \chi_{tot}^2 + k \ln N$ , where  $k$  is the number of parameters and  $N$  the number of data points. Our dark energy model and LCDM have  $AIC = 1605.8 + 12 = 1617.8$ ,  $BIC = 1664.3$  while the best  $w(z)$  has  $AIC = 1622.9$ ,  $BIC = 1676$ . We see that for both criteria our dark energy models has a better fit than the best effective  $w(z)$  model and an equivalent fit as LCDM. The evolution of our dark energy model and  $\sigma_8$  lie at the central values obtained in [4]-[6].

As a matter of completeness we have determined the best fit if the exponential factor in eq.(1) is not present (i.e. for  $V = c^2 \Lambda_c^{4+2/3} \phi^{-3/2}$ ). In this case we get for  $\Omega_{DGi} = 0.11$  a  $P_5 = (69, 0.71, 0.0228, 0.12, 0.97)$  giving  $\chi_{tot}^2 = \chi_{sn1a}^2 + \chi_{wmap}^2 = 177.7 + 1428.9 = 1606.6$  with  $\chi_{tot}^2/dof = 1.08$  and an equivalent fit as before.

To see the difference between our dark energy model compared to LCDM we have calculated the CMB using the same  $P_6$  in both cases. For small  $\Omega_{DGi}$  (i.e.  $\Omega_{DGi} = 0.01, 0.03$ ) we get a variation of about 0.2–0.5% increase in the three peaks while an increase of about 1–3% at lower multipoles with a resulting  $\Delta\chi_{wmap}^2 \simeq 10$  in favor of our dark energy model. On the other hand for  $\Omega_{DGi} = 0.06$  or 0.11 the variation is much smaller, less than 0.05%, giving, therefore, an equivalent  $\chi_{wmap}^2$ . However, by changing  $P_6$  we can get an equivalent fit for LCDM as for our dark energy models. The ISW effect for a dynamical  $w(z)$  gives a nontrivial (but small) imprint on the power spectrum [5] but this contribution can be taken into account by a change in  $P_6$ . The great degeneracy on the cosmological parameters  $P_6$  reduces

the possibility of distinguishing between different dark energy models at present time. The LSS data do not place a stronger constraint on the evolution of dark energy than the SN1a and wmap data [4]-[6]. Without an independent way of measuring  $P_6$  it is hard to distinguish from the data between different dark energy models and we should choose the best theoretical model.

Let us conclude. We have presented a realistic dark energy model derived from particle physics that has essentially no free parameters. The reason why the universe accelerates at such a late time is because the dark energy (quintessence field) appears at a very late time due to the gauge group dynamics. Our model has a almost flat  $w$ , with  $-1 < w_o < -0.94$ , and has a better fit to the cosmological observations than the best  $w(z)$  effective model and an equivalent fit than LCDM. Unfortunately the great degeneracy on the cosmological parameters  $P_6$  reduces the possibility of distinguishing between different dark energy models from the observations. Therefore, we are left, at present time, with the most appealing theoretical model as the best candidate for dark energy. This is the model with the least number of free parameters and with the best explanation of the origin of dark energy and its late time appearance. Our dark energy model satisfies these criteria.

#### Acknowledgments

We would like to thank P.S. Corasaniti for making KINKFAST1.0.1 available and for useful discussions. This work was supported in part by CONACYT project 45178 and DGAPA, UNAM project IN-110200.

- 
- [1] C.L. Bennet et al., *Astrophys. J. Suppl.* 148 (2003) 1
  - [2] A.G. Riess et al., *Astrophys. J.* 607 (2004) 665
  - [3] K.Abazajain et al. *Astron.J.*128(2004)502
  - [4] Max Tegmark et al., *Phys.Rev.D*69:103501,2004
  - [5] P.S. Corasaniti, M.Kunz, D.Parkinson, E.J. Copeland and B.A. Bassett, astro-ph/0406608
  - [6] U. Seljak et al., astro-ph/0407372
  - [7] B. Ratra and P.J.E. Peebles *Phys.Rev.D*37 (1988) 3406
  - [8] P. Binetruy, *Phys.Rev. D*60 (1999) 063502; A. Masiero, M. Pietroni and F. Rosati, *Phys. Rev. D*61 (2000) 023504
  - [9] I.Affleck, M.Dine, N.Seiberg, *Nucl.Phys.B*256(1985)557
  - [10] A. de la Macorra and C. Stephan-Otto, *Phys.Rev. Lett.*87:271301,2001; *Phys.Rev.D*65:083520,2002
  - [11] A. de la Macorra *JHEP* 0301(2003)033(hep-ph/0111292); *Phys.Rev. D*67 (2003) 103511(astro-ph/0211519)
  - [12] R.Bean, S.H.Hansen, A.Melchiorri,*Phys.Rev.D*64(2001) 103508
  - [13] V.Barger, J.P.Kneller, P.Langacker, D.Marfatia, G.Steigman, *Phys.Lett. B*569(2003)123
  - [14] G.F. Giudice, R. Rattazzi, *Phys.Rept.*322:(1999) 419
  - [15] KINKFAST1.0.1, P.S. Corasaniti
  - [16] U.Seljak and M. Zaldarriaga, *Astrophys. J.*469(1996)437
  - [17] H.Akaike, *IEEE Trans.Auto.Control*, 19 (1974) 716
  - [18] G. Schwarz, *Annals of Statistics*, 5, (1978) 461